



Interfacial adsorption of Ca^{2+} and Mg^{2+} from high salinity wastewater by layered double oxides

Xiaoxia Zhang, Yiqian Cheng, Jixin Su*, Guoqing Wang, Luyao Wang, Yuxin Xiao, Xue Gao

School of Environmental Science and Engineering, Shandong University, Jinan 250100, China, Tel./Fax: +86-531-88362008; emails: 907197606@qq.com (J. Su), zxx120468@163.com (X. Zhang), 1403709770@qq.com (Y. Cheng), 1473595461@qq.com (G. Wang), 609475978@qq.com (L. Wang), 17862923736@163.com (Y. Xiao), amberwonder@outlook.com (X. Gao)

Received 31 August 2017; Accepted 12 February 2018

ABSTRACT

The removal of Ca^{2+} and Mg^{2+} in saline wastewater is a significant environmental problem. In this paper, an innovative way to remove Ca^{2+} and Mg^{2+} ions by Mg–Al layered double oxides (LDOs) was studied. During the process, the adsorption of Ca^{2+} and Mg^{2+} was synchronous with the lattice reconstruction of Mg–Al layered double hydroxides (LDHs). The study found that adsorption isotherm at four experimental temperatures follows the Langmuir isotherm model. The maximum Ca^{2+} and Mg^{2+} adsorption capacities were 305.31 and 105.99 mg/g, respectively. The thermodynamic parameters calculated from the temperature-dependent isotherms indicated that the adsorption was a spontaneous and endothermic process, and the adsorption kinetics followed the pseudo-second-order model. Certain competitive and mutually promoted effects were observed during the Ca^{2+} and Mg^{2+} adsorption process in the binary ion system. Regeneration experiment showed that LDOs have excellent repeatability. The removal percentage of Ca^{2+} and Mg^{2+} in actual desulfurization wastewater can reach more than 70%. Further, the results of X-ray diffraction and scanning electron microscopy indicated that the structure of hydroxalite lamellae collapsed after calcination, though the structure of hydroxalite gradually recovered through a series of chemical reactions with the adsorption of Ca^{2+} or Mg^{2+} and the insertion of anion during the adsorption process.

Keywords: Mg–Al layered double oxides; Saline wastewater; Adsorption; Reconstruction; Repeatability

1. Introduction

Heavy metal ions in wastewater received significant research attention due to their toxicity [1]. However, only limited attention has been given to salinity of wastewater, although strict environmental regulations exist for controlling the total salinity. With increased awareness of climate change, water pollution and other environmental issues, the relevant environmental protection standards have become more stringent. The salinity in sewage is already an important indicator in the emission standards. In recent years, increased demand for electricity has led to excessive SO_2 emission from

coal-fired power plants and caused severe smog in many areas of China. To meet the strict emission standards [2], wet limestone-gypsum flue gas desulfurization process has been widely used for the removal of SO_2 [3] and for the prevention of haze. The desulfurization produces saline wastewater that would require desalination treatment before discharge. Unfortunately, the calcium, magnesium and sulfate ions in the saline wastewater are significantly higher for traditional reverse osmosis and evaporation operations [4]. In addition, ion exchange or membrane separation method is suitable only for the tertiary treatment of drinking water and other low salinity water, while they are inappropriate for the treatment of wastewater with high calcium and magnesium. It is worthy to note that non-toxic ions such as Ca^{2+} and Mg^{2+} can

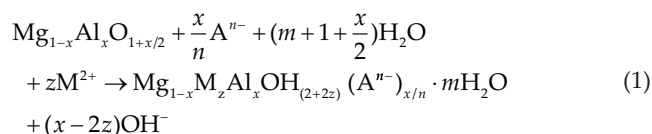
* Corresponding author.

cause scaling and blockage in the equipment when desalting the industrial wastewater with high calcium and magnesium. Therefore, it is important to remove Ca^{2+} and Mg^{2+} before further processing the highly saline wastewater treatment. This aspect is also an innovative outcome of this study.

Various methods such as extraction, ion exchange, adsorption, membrane filtration, chemical precipitation and biological treatment [5,6] have been investigated for the removal of metal ions from wastewater. Among them, the adsorption method was found to be efficient and environmentally benign [7]. Compared with other adsorbents such as cork bark and grape stalks wastes, layered double hydroxides (LDHs) are more efficient, economical and non-toxic with special layered structure and large specific surface area. Additionally, they are easy to prepare. Therefore, LDHs have been extensively utilized as efficient adsorption materials for adsorbing various anions [8,9] and metal cations [10].

Several modifications have been proposed for LDHs to improve their adsorption capacity. Some studies investigated the use of LDHs modified with humate, ammonium sulfate and dodecyl sulfate for metal adsorption [11,12], and found limited increase in the adsorption efficiency compared with LDHs. Similarly, calcined LDHs (layered double oxides [LDOs]) possess higher specific surface area and well developed pore distribution than the pristine hydroxaltes. Moreover, LDOs have good regeneration capacity. LDOs exhibit superior adsorption capacities for anionic ions than LDHs in aqueous solutions, which had been confirmed in many previous studies [13]. In recent years, because of its memory effect and surface alkalinity, the adsorption of metal cations by LDOs has received significant research attention [14]. It has been reported that the study of the adsorption mechanism focuses on the combined action of surface adsorption and surface precipitation and the memory effect of LDOs [15]. Therefore, the material has excellent adsorption properties. Thus, the adsorption of Ca^{2+} and Mg^{2+} by LDOs was investigated in this study.

The LDO samples can transform to their original structures of LDHs in aqueous solution if calcined below 550°C [16] due to the structure memory effect [17]. LDHs are anionic clays, also known as hydroxaltes compounds. They are represented by the general formula of $[\text{M}_{1-x}^{\text{II}}\text{M}_x^{\text{III}}(\text{OH})_2]^{x+}(\text{A}^{n-})_{x/n} \cdot m\text{H}_2\text{O}$ [18]. The structure consists of brucite-like layers with a x positive charge due to the substitution of trivalent metal cations M^{III} for bivalent metal cations M^{II} . These layers are balanced by an equivalent interlayered negative charge $(\text{A}^{n-})_{x/n}$, where n is the negative charge of anion [19]. Using Mg–Al hydroxaltes as an example, the uptake process of divalent cations (M^{2+}) on LDOs can be represented by the following formula [14]:



Ca^{2+} and Mg^{2+} are important factors that affect the function of water bodies. Treatment of saline wastewater with

high hardness is of a great significance. This paper is one of the few studies on the removal of hardness in wastewater by adsorption. Due to the large surface area, high porosity and specific structure, LDOs have been extensively utilized as efficient adsorption materials for adsorbing various anions and heavy metal ions but only limited attention has been given to the treatment of hardness of high salinity wastewater by LDOs. Therefore, in this study, the Ca^{2+} and Mg^{2+} adsorption capacities of Mg–Al LDOs were investigated. Adsorption kinetics, isotherms, thermodynamics and competitive adsorption were also studied. Further, the adsorption mechanisms were analyzed in detail using X-ray diffraction (XRD), scanning electron microscopy (SEM), the Brunauer–Emmett–Teller (BET) method and electron dispersive X-ray analysis (EDX).

2. Materials and methods

2.1. Materials

The chemicals, $\text{Mg}(\text{NO}_3)_2 \cdot 6\text{H}_2\text{O}$, $\text{Al}(\text{NO}_3)_3 \cdot 9\text{H}_2\text{O}$, NaOH and Na_2CO_3 , CaCl_2 and $\text{MgCl}_2 \cdot 6\text{H}_2\text{O}$, were of analytical reagent grade and used as received without further purification. Deionized and ultrapure water were used in all experiments. The synthetic magnesium and calcium chloride solutions (concentration: 10,000 mg/L) were used as stock solutions. The pH was adjusted using pre-determined volumes of 0.1 M HNO_3 and 0.185 M Na_2CO_3 solutions.

2.2. Synthesis of Mg–Al LDHs and Mg–Al LDOs

The well-crystallized $\text{Mg}_3\text{Al}-\text{CO}_3$ LDHs were prepared using the co-precipitation method [20]. Solution A was prepared by mixing 15.3 g of $\text{Mg}(\text{NO}_3)_2 \cdot 6\text{H}_2\text{O}$ and 7.5 g of $\text{Al}(\text{NO}_3)_3 \cdot 9\text{H}_2\text{O}$ at a $\text{Mg}^{2+}/\text{Al}^{3+}$ molar ratio of 3:1 in 200 mL deionized water. Solution B was prepared by mixing 1.6 mol of NaOH and 0.1 mol of Na_2CO_3 in 250 mL deionized water. Solutions A and B were added dropwise to a vessel containing deionized water (400 mL) under vigorous stirring. Meanwhile, the pH of the mixture was controlled at 10 ± 0.5 [21]. After stirring for 2 h, the precipitate was separated by vacuum filtration, and then was aged at 80°C for 24 h to obtain LDHs. Calcination of Mg–Al LDHs (Mg–Al LDOs) was carried out in a muffle furnace at 450°C for 2 h to prepare calcined samples.

2.3. Adsorption kinetics

Kinetics experiments were carried out in a thermostat shaker at a constant speed of 150 rpm at 25°C , 35°C , 45°C and 50°C . The initial concentration of Ca^{2+} and Mg^{2+} in saline solution was 500 mg/L, the volume of solution was 100 mL, and the sorbent dosage was 1 g/L. The initial pH of the Mg^{2+} solution was about 9 and was adjusted using 0.185 M Na_2CO_3 . However, the initial pH of Ca^{2+} solution was neutral without adjustment. A 2 mL supernatant liquid was taken for centrifugation at 0, 10, 30, 50, 90, 120, 180, 240 and 300 min time intervals. They were filtered through 0.22 μm membrane, and the filtrates were analyzed by the flame atomic absorption spectrophotometer (TAS-990).

The Ca^{2+} and Mg^{2+} adsorption capacities of LDOs were calculated using the following formula:

$$q_{t,e} = (C_0 - C_{t,e})V/m \quad (2)$$

where $q_{t,e}$ is the sorption capacity of adsorbent at the time t or equilibrium (mg/g), V is the volume of solution in L, m is the mass of LDOs in g, C_0 is the initial concentration of Ca^{2+} and Mg^{2+} (mg/L) and $C_{t,e}$ is the concentration at t (min) or equilibrium (mg/L) [12,22].

2.4. Adsorption equilibrium

The isotherms for Ca^{2+} and Mg^{2+} sorption by LDOs were performed at different temperatures (25°C, 35°C, 45°C and 50°C) at the initial Ca^{2+} concentrations of 200, 400, 600, 800 and 1,000 mg/L, and at the initial Mg^{2+} concentration of 100, 200, 300, 400 and 500 mg/L for 300 min contact time at 150 rpm. The test method was same as before, except for the adsorption time.

2.5. Competitive adsorption study

The solutions were prepared with a mixture of $\text{Ca}^{2+} + \text{Mg}^{2+}$ (500 mg/L + 500 mg/L). The volume of solution was 100 mL and the sorbent dosage was 1 g/L. The initial solution pH was about 8 and was adjusted using 0.185 M Na_2CO_3 . The test temperature was set at 35°C. A 2 mL supernatant liquid was taken for centrifugation at 0, 10, 30, 50, 90, 120, 180, 240 and 300 min time intervals. They were filtered by 0.22 μm membrane and the filtrates were analyzed using the flame atomic absorption spectrophotometer [23].

2.6. Reusability and application in actual wastewater

To determine the reusability of the adsorbent, adsorption/calcinations cycles were repeated five times using the same LDO sample. Adsorbent (600 mg) was placed in 100 mL of Ca^{2+} (or Mg^{2+}) solution at the concentration of 500 mg/L at the temperature of 308.15 K for 5 h, every time.

The Ca^{2+} or Mg^{2+} removal percentage was calculated using the following equation [24]:

$$\text{Removal}(\%) = \frac{C_0 - C_t}{C_0} \times 100\% \quad (3)$$

where C_0 (mg/L) and C_t (mg/L) are the Ca^{2+} or Mg^{2+} concentrations at the beginning and at time t , respectively.

The treatment of actual desulfurization wastewater from a coal-fired power plant by LDOs was also studied. The adsorption experiment was conducted soon after taking water sample. The wastewater was first filtered through 0.25 μm membrane to remove the suspended solids. Since this study mainly investigated the removal of Ca^{2+} and Mg^{2+} , initial concentrations of Ca^{2+} (1,620.5 mg/L) and Mg^{2+} (3,066.4 mg/L) were measured. The original pH of actual wastewater was measured about 8.45 because of the previous traditional treatment. The experiment was carried out for 5 h at 30°C to calculate the Ca^{2+} or Mg^{2+} removal rate.

2.7. Characterization

XRD patterns for the prepared samples were recorded using a Rigaku D/MAX-RA instrument with $\text{Cu K}\alpha$ radiation ($\lambda = 0.154184$ nm) at 40 kV and 50 mA in the 2θ range of 2° – 70° with a scanning rate of $8^\circ/\text{min}$. The specific surface area was measured using N_2 adsorption/desorption at 77 K using a Quantachrome SI system. The pore-size distributions of samples were calculated from desorption curve according to the Barrett–Joyner–Halenda method [20]. SEM images and EDX were produced using the Hitachi S-4800 microscope and EDAX instruments, respectively [25].

3. Results and discussion

3.1. Characterization of LDOs

Fig. 1 shows the XRD patterns of uncalcined and calcined LDHs. Mg–Al LDHs exhibited characteristic reflections of 003, 006, 012 and 110 at $2\theta = 11.41^\circ$, 23.42° , 36.31° and 60.74° with intense and sharp reflections, indicating that the material consisted of a single crystalline phase and was well crystallized [26,27]. For calcined hydrotalcites, the characteristic peaks (003) and (006) of hydrotalcites disappeared [28]. The reflections of MgO at $2\theta = 42.60^\circ$ and 62.50° can be observed, suggesting that the layered octahedral structure of LDHs was destroyed, while the anions and interlayer water disappeared, and was composed of mixed oxide of Mg(Al)O.

Typical N_2 adsorption and desorption isotherms, along with the pore size distributions of the LDHs and LDOs are shown in Fig. 2. The adsorption–desorption isotherms followed a type IV according to the IUPAC classification with H_3 hysteresis loop, suggesting that the material was mesoporous [29]. The N_2 adsorption–desorption isotherms show that the LDOs had larger mesoporous pore diameter than LDHs. Further, the BET surface area of LDHs was 102.655 m^2/g , while that of LDOs was 206.901 m^2/g [30]. Evidently, LDOs had a larger surface area, which could offer more active adsorption sites, leading to a better ability to adsorb metal ions.

As shown in Fig. 3, the SEM image of LDHs presented well-developed layered structure with fine dispersion of the alveolate-like particles [31,32]. In terms of LDOs, there were

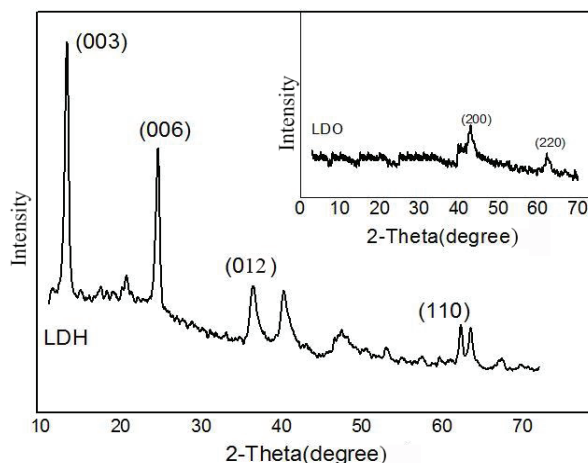


Fig. 1. XRD patterns for LDHs and LDOs.

no flakiness structures, and the samples were close-knit and rough contrarily, because of the collapse of the LDHs layer sheet structure after the calcination.

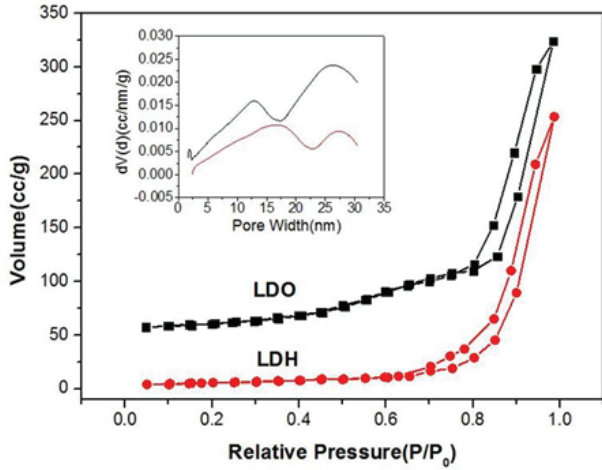


Fig. 2. N₂ adsorption–desorption isotherms and pore size distribution (inset) of LDOs and LDHs.

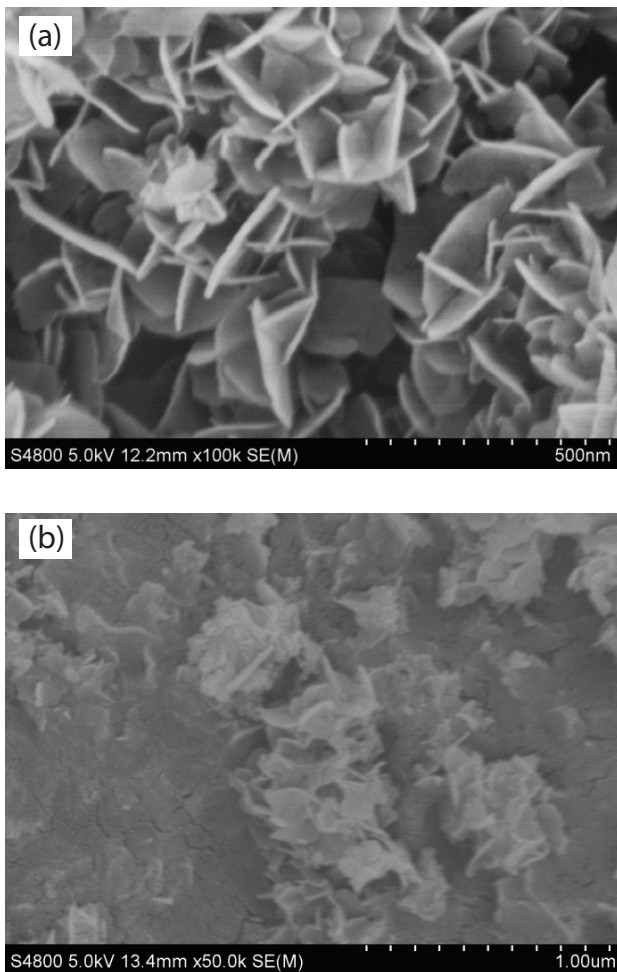


Fig. 3. Scanning electron microscopy images of uncalcined (a) and calcined (b) MgAl LDHs.

3.2. Adsorption kinetics

The variation in the amount of Ca²⁺ and Mg²⁺ adsorbed by LDOs as a function of contact time (0–300 min) at different temperatures is shown in Fig. 4. Evidently, the adsorption of Ca²⁺ and Mg²⁺ increased rapidly in the first 50 and 30 min, respectively, before slowing down and gradually reaching saturation [33]. In addition, the uptake of Ca²⁺ or Mg²⁺ by LDOs increased with increasing temperature, indicating that a higher temperature is beneficial to improve the adsorption process [34,35]. It is hypothesized that the adsorption of Ca²⁺ or Mg²⁺ by LDOs is an endothermic process; thus, more active sites are available in the adsorbents at higher temperatures.

To further investigate the adsorption behaviors for Ca²⁺ and Mg²⁺ by calcined hydrotalcites, the following three well-known kinetic equations, namely pseudo-first-order [36], pseudo-second-order [37,38] and intraparticle diffusion [13] models were used:

$$\ln(q_e - q_t) = \ln q_e - k_1 t \tag{4}$$

$$t/q_t = 1/(k_2 q_e^2 + t/q_e) \tag{5}$$

$$q_t = k_i t^{0.5} \tag{6}$$

where q_t and q_e (mg/g) are the amounts of metal ions adsorbed per unit mass of the adsorbents at time t and at equilibrium, respectively, k_1 (min⁻¹), k_2 (g/mg min) and k_i

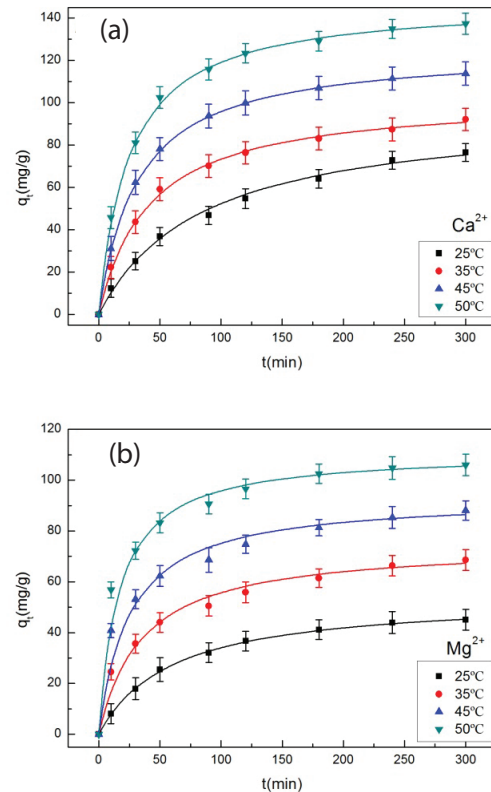


Fig. 4. Kinetics of (a) Ca²⁺ and (b) Mg²⁺ adsorption on LDOs from aqueous solution at different temperatures. Solid lines represent predicted data by pseudo-second-order.

(mg/g min^{0.5}) are the rate constants of the pseudo-first-order, pseudo-second-order and intraparticle diffusion models. The parameters and the correlation coefficients are presented in Table 1. As evident in Table 1, the correlation coefficients (R^2) of the pseudo-second-order kinetics model are larger than that of the other two models for both ions. Furthermore, the $q_{e,cal}$ obtained from the pseudo-second-order kinetics model is closer to the experimental values ($q_{e,exp}$), suggesting that the pseudo-second-order kinetics model could better describe the Ca^{2+} and Mg^{2+} adsorption process by LDOs. These results show that chemisorption could have dominated the adsorption process [14,39]. Furthermore, rate constant, K_2 , and the equilibrium capacity for Ca^{2+} or Mg^{2+} increased with increasing temperatures (298–323 K), which also indicate that the increasing the temperature is favorable for adsorption process.

To understand the rate constant, K_2 , and the influence of temperature on the adsorption process, the following Arrhenius equation, defined as an empirical formula of the relationship between chemical reaction rate constant and temperature, was used [40]:

$$K_2 = A \exp(-E_a/RT) \tag{7}$$

$$\ln K_2 = \ln A - E_a/RT \tag{8}$$

where E_a (kJ/mol) is the activation energy, R (8.314 J/mol·K) is molar gas constant and A [g/(mg min)] is the pre-exponential factor. The adsorption activation energy (E_a) for Ca^{2+} and Mg^{2+} calculated based on $\ln K_2$ vs. $1/T$ plot is presented in Table 2. As evident in Table 2, the activation energy (E_a) for Ca^{2+} and Mg^{2+} is greater than 20 kJ/mol, indicating that the Ca^{2+} or Mg^{2+} adsorption process was similar and controlled by the reaction rate of metal ions adsorbed on LDOs rather

than by diffusion [16,41]. Thus, it can be concluded that process of Ca^{2+} or Mg^{2+} removal by LDOs is chemical adsorption.

3.3. Adsorption isotherm

Adsorption isotherms are mathematical models that were used to determine the Ca^{2+} and Mg^{2+} removal capacities of LDOs. For the liquid–solid system, the Langmuir and Freundlich equilibrium models are generally used [17], and the corresponding isotherm equations are given as follows [42,43]:

$$C_e/q_e = 1/q_m K_L + C_e/q_m \tag{9}$$

$$\ln q_e = \ln K_F + 1/n \ln C_e \tag{10}$$

where C_e is the equilibrium metal ion concentration in the solution (mg/L), q_m (mg/g) is the maximum adsorption capacity, K_L (1/mg) is the Langmuir isotherm constant, and K_F and n are the Freundlich constants related to the adsorption capacity and intensity of adsorption, respectively. The plots for the Langmuir model for Ca^{2+} and Mg^{2+} adsorption by LDOs at 298–323 K are shown in Fig. 5. It can be concluded that the metal ion adsorption process is explained better by the Langmuir model with $R^2 > 0.99$ (Table 3) [32], suggesting that active sites were generally distributed uniformly on the surface of LDOs and the adsorption process was monolayer adsorption [44,45]. Furthermore, as per Fig. 5, the adsorption capacity increased with increasing equilibrium concentrations of Ca^{2+} and Mg^{2+} . For the same equilibrium concentration, the amounts of Ca^{2+} and Mg^{2+} increased with increasing temperature, which is in agreement with the outcomes of kinetic study results. Therefore, the Ca^{2+} and Mg^{2+} adsorption capacities of LDOs were the maximum when initial Ca^{2+} and

Table 1
Kinetic constants of Ca^{2+} or Mg^{2+} adsorption on LDOs for initial concentrations of 500 mg/L at different temperatures and analyzed by different models

	T (K)	$q_{e,exp}$ (mg/g)	Pseudo-first-order			Pseudo-second-order			Intraparticle diffusion	
			$q_{e,cal}$ (mg/g)	k_1 (min ⁻¹)	R^2	$q_{e,cal}$ (mg/g)	k_2 (g/mg min)	R^2	k_i	R^2
Ca^{2+}	298.15	76.5289	76.8066	0.01154	0.9715	96.1538	1.257E-04	0.9912	4.62644	0.9885
	308.15	92.1	72.4075	0.01185	0.9765	102.669	2.250E-04	0.9990	5.27914	0.9197
	318.15	113.8218	89.9820	0.01516	0.9860	125.313	2.636E-04	0.9999	6.4835	0.8803
	323.15	137.31	98.8615	0.01528	0.9703	147.710	2.868E-04	0.9998	7.5252	0.8438
Mg^{2+}	298.15	45.0584	44.3437	0.01458	0.9894	54.113	3.190E-04	0.9994	2.74933	0.9522
	308.15	68.6027	54.5229	0.01256	0.9736	74.850	4.081E-04	0.9939	3.72265	0.9206
	318.15	88.0607	60.3759	0.01279	0.9671	93.371	5.050E-04	0.9958	4.49023	0.8503
	323.15	105.9862	67.4253	0.01676	0.9737	110.988	6.199E-04	0.9989	5.23046	0.7627

Table 2
Relevant parameters of the activation energy for Ca^{2+} or Mg^{2+} adsorption on LDOs at different temperatures

	E_a (kJ/mol)	$\ln A$	$\ln K_2$				R^2
			298 K	308 K	318 K	323 K	
Ca^{2+}	25.099	1.238	-8.982	-8.400	-8.241	-8.157	0.8344
Mg^{2+}	20.167	0.0733	-8.047	-7.804	-7.591	-7.386	0.9774

Mg²⁺ concentrations were 1,000 and 500 mg/L, respectively, reaction time was 300 min, and the temperature was 323.15 K. Additionally, LDOs had higher affinity for Ca²⁺ adsorption than Mg²⁺ adsorption.

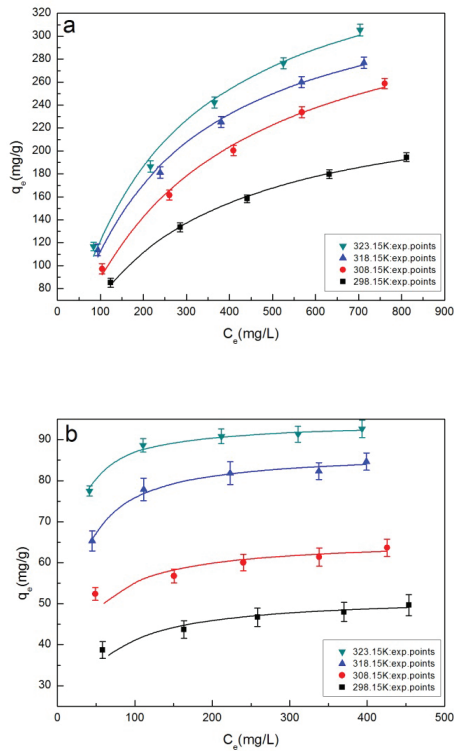


Fig. 5. The adsorption isotherms of (a) Ca²⁺ and (b) Mg²⁺ on LDOs at different temperatures. Solid lines represent predicted data by Langmuir model.

Table 3

Isotherm parameters obtained using a linear method for the adsorption of Ca²⁺ and Mg²⁺ on LDOs at different temperatures

	Langmuir adsorption model				Freundlich adsorption model		
	T (K)	Q _{max} (mg/g)	K _L (L/mg)	R ²	K (mg/g) (L/mg) ^{1/n}	n	R ²
Ca ²⁺	298	252.5253	0.00397	0.9986	10.6615	2.2789	0.9833
	308	355.8719	0.00336	0.9938	9.8947	2.0117	0.9935
	318	359.7122	0.00457	0.9936	15.4913	2.2492	0.9902
	323	396.8254	0.00446	0.9964	15.6123	2.1807	0.9930
Mg ²⁺	298	51.8403	0.03914	0.9985	23.7177	8.2994	0.9952
	308	65.48789	0.05443	0.9981	36.9021	11.3096	0.9812
	318	87.0322	0.06935	0.9995	44.1516	9.0277	0.8788
	323	94.3396	0.11901	0.9999	59.7859	13.1874	0.8499

Table 4

Thermodynamic data for adsorption of Ca²⁺ or Mg²⁺ onto LDOs at temperatures ranging from 298 to 323 K

	ΔH (kJ/mol)	ΔS (kJ/mol K)	ΔG (kJ/mol)			
			298 K	308 K	318 K	323 K
Ca ²⁺	19.036	0.0645	-0.1850	-0.8300	-1.4750	-1.7975
Mg ²⁺	51.487	0.17802	-1.56296	-3.34316	-5.12336	-6.01346

3.4. Adsorption thermodynamics

The thermodynamic parameters were analyzed to investigate the inherent energetic changes during adsorption [46]. The following thermodynamic parameters such as changes in Gibbs free energy (ΔG°, kJ/mol), enthalpy (ΔH°, kJ/mol) and entropy (ΔS°, kJ/mol/K) [38,40,47,48] were used (Table 4 and Fig. 6):

$$\Delta G^\circ = \Delta H^\circ - T\Delta S^\circ \quad (11)$$

$$\Delta G^\circ = -RT\ln K_D \quad (12)$$

$$\ln K_D = \Delta S^\circ/R - \Delta H^\circ/RT \quad (13)$$

$$K_D = q_d/c_e \quad (14)$$

where T is absolute temperature (K), K_D is the distribution coefficient and R is the standard molar gas constant (8.314 J/mol K).

The negative values of ΔG° (Table 4) indicate that the adsorption by LDHs was a spontaneous process. In addition, ΔG° decreased with increasing temperature, that is, the spontaneous adsorption process is easier at higher temperature. The positive ΔH° shows that the adsorption process was endothermic [44], while the positive ΔS° indicates an increased randomness at the solid/solution interface during the adsorption process [12]. According to the ΔG° and ΔS° for Ca²⁺ and Mg²⁺, the LDOs had higher affinity for Ca²⁺ than Mg²⁺. The results confirm that adsorption rate and uptake capacity of Ca²⁺ or Mg²⁺ increase with increasing temperature [46], which is in agreement with the outcomes of the kinetic study (Fig. 4 and Table 1). The symbols in all equations is listed in Table 7.

3.5 Competitive adsorption

The three kinetic models (Eqs. (4), (5), and (6)) were used to investigate the potential co-adsorption mechanism for Ca^{2+} and Mg^{2+} . As evident in Table 5 and Fig. 7, adsorption of the binary system is in accordance with the pseudo-second-order model. The rate constant, K_2 , for Ca^{2+} in

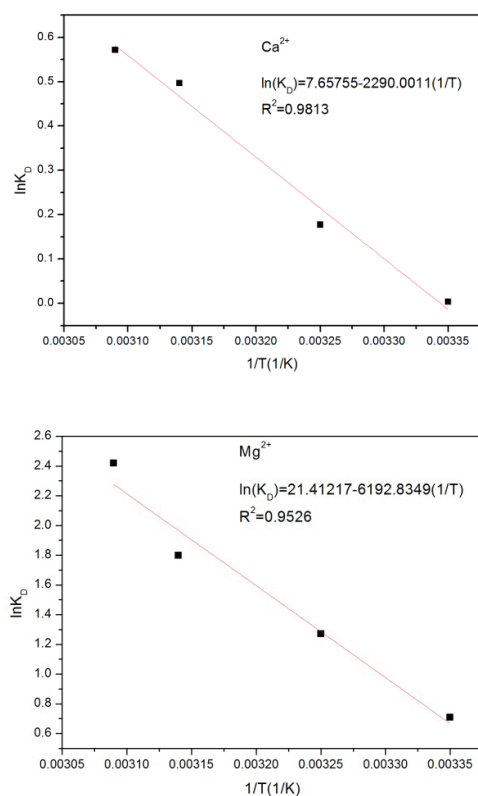


Fig. 6. Van't Hoff plot for adsorption of Ca^{2+} or Mg^{2+} by LDOs.

Table 5

Kinetic parameters of pseudo-first-order, pseudo-second-order and intraparticle diffusion models at test temperature (308.15 K) for Ca^{2+} and Mg^{2+} in single/binary systems

$q_{e,exp}$ (mg/g)	Pseudo-first-order			Pseudo-second-order			Intraparticle diffusion		
	$q_{e,cal}$ (mg/g)	k_1 (min^{-1})	R^2	$q_{e,cal}$ (mg/g)	k_2 (g/mg min)	R^2	k_i	R^2	
Single system									
Ca^{2+}	92.1	72.4075	0.01185	0.9765	102.669	2.250E-04	0.9990	5.27914	0.9197
Mg^{2+}	68.6027	54.5229	0.01256	0.9736	74.850	4.081E-04	0.9939	3.72265	0.9206
Binary system									
Ca^{2+}	78.5	60.1878	0.01131	0.9681	86.655	3.043E-04	0.9977	4.42243	0.9118
Mg^{2+}	61.9821	50.0684	0.01212	0.9787	68.729	3.772E-04	0.9972	3.49634	0.9279

Table 6

Investigation on the effective treatment of actual desulfurization wastewater by MgAl LDOs

Type of wastewater	Ions	Initial concentration (ppm)	Equilibrium concentration (ppm)	Removal (%)
Desulfurization wastewater	Ca^{2+}	1,620.5	450.7	72.2
	Mg^{2+}	3,066.4	637.5	79.2

the single system is 2.250×10^{-4} g/mg min, while it increased to 3.043×10^{-4} g/mg min in the binary system. However, the Mg^{2+} adsorption constant decreased from $\sim 4.081 \times 10^{-4}$ g/mg min to $\sim 3.772 \times 10^{-4}$ g/mg min. Hence, during the co-adsorption of Ca^{2+} and Mg^{2+} , the adsorption was more favorable for Ca^{2+} than Mg^{2+} . In addition, the total Ca^{2+} and Mg^{2+} adsorption capacities in the binary system were larger than those in single systems, although the equilibrium Ca^{2+} and Mg^{2+} adsorption capacities in the single system were 92.10 and 68.60 mg/g, respectively, which reduced to 78.50 and 61.98 mg/g in the binary system. As such, mutual promotion existed between Ca^{2+} and Mg^{2+} in the binary adsorption system. Therefore, the simultaneous removal of Ca^{2+} and Mg^{2+} in wastewater is possible. Further, the results show that Ca^{2+} and Mg^{2+} competed for the limited number of active sites of LDOs with an equal binding force [49,50].

3.6 Reusability and application in actual wastewater

It is of great economic value to evaluate the regenerative behavior of the adsorbents. The adsorption of Ca^{2+} or Mg^{2+} using LDOs regenerated after treatment at 308 K for five times is shown in Fig. 8. It can be concluded that most Ca^{2+} and Mg^{2+} could be removed under the experimental conditions during the first three adsorption processes. In addition, the removal efficiency can still reach more than 50% in the fifth time. These results indicate that LDOs could be efficiently recycled to remove Ca^{2+} and Mg^{2+} in solutions. The decrease in the adsorption efficiency can be attributed to the decrease in the crystallinity of the recycled adsorption material and the gradual decrease of the available adsorption sites with increased number of cycles [14,51]. The total amount of Ca^{2+} and Mg^{2+} removed was 360.08 and 312.55 mg/g, respectively. Table 6 shows the characteristics of actual desulfurization saline wastewater from a coal-fired power plant. It can be concluded that the removal of Ca^{2+} or Mg^{2+} in actual desulfurization wastewater can reach more than 70%. The equilibrium Ca^{2+} and Mg^{2+} concentrations

were 450.7 and 637.5 mg/g, respectively, which can ensure zero discharge of desulfurization wastewater through further processing with reverse osmosis and evaporation. The adsorption of heavy metal ions by LDOs has been investigated in the previous studies [14,21]. The co-adsorption of trace heavy metal ions, Ca^{2+} and Mg^{2+} in actual desulfurization wastewater can be achieved. Thus, Mg–Al LDOs as sorbent is valuable for practical applications [8,32].

3.7. Adsorption mechanism

The above experiments indicated that the Ca^{2+} and Mg^{2+} adsorption processes by LDOs are endothermic and spontaneous chemical adsorption. To further understand the

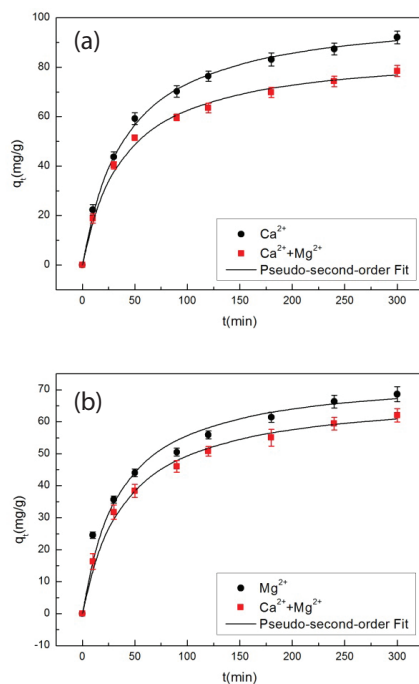


Fig. 7. Pseudo-second-order models fit for (a) Ca^{2+} and (b) Mg^{2+} adsorption by LDOs ($[\text{Ca}^{2+} + \text{Mg}^{2+}] = 500 \text{ mg/L} + 500 \text{ mg/L}$).

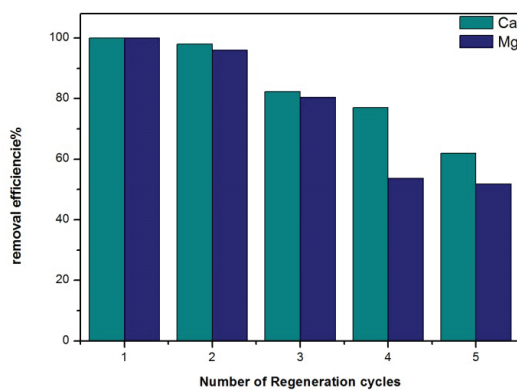


Fig. 8. Removal efficiency of Ca^{2+} or Mg^{2+} in different cycles by using LDOs ($[\text{Ca}^{2+}] = [\text{Mg}^{2+}] = 500 \text{ mg/L}$, $T = 35^\circ\text{C}$; LDOs = 0.6 g/100 mL).

mechanism as shown in Fig. 13, the change in pH in the solution and the characteristics of the sample before and after the adsorption were measured. The solution pH variation was studied at the kinetic adsorption condition at 35°C . As evident in Fig. 9, the initial pH of Mg^{2+} solutions was adjusted with Na_2CO_3 to about 9. However, for Ca^{2+} , the pH was not adjusted. The possible mechanism can be hydrolysis reaction occurred on the surface of adsorbent, when the particles of Mg–Al LDOs were exposed to aqueous solutions. Consequently, hydroxyl ions were released and pH rapidly increased (Fig. 9), leading to the formation of calcium and magnesium hydroxide attached on the surface of adsorbent because of the high OH^- solution gradient. Several studies have investigated the heavy metal adsorption mechanism of LDOs. Heavy metal ions easily precipitated as their hydroxides because of the low relative stability and transferred from water to solid phase. During the adsorption process, precipitates could not be observed in solutions, though heavy metal ions were largely removed according to the kinetics experiment. Due to the high relative stability of calcium hydroxide ($K_{\text{sp}} = 5.5 \times 10^{-6}$) and magnesium hydroxide ($K_{\text{sp}} = 1.8 \times 10^{-11}$), the removal process tends to be surface adsorption. The effect of surface precipitation deposition was eliminated effectively reflecting the intrinsic adsorption properties of the material. Ca^{2+} , Mg^{2+} and Al^{3+} were released because of the ionization of hydroxide, and combined with the hydroxyl again to form octahedral lamellar structure. Because of the existence of trivalent cations Al^{3+} , the sheets had a resultant positive charge. The above reactions proceeded on the new adsorbent surface in oxide state. Thus, a mass of metal ions was removed

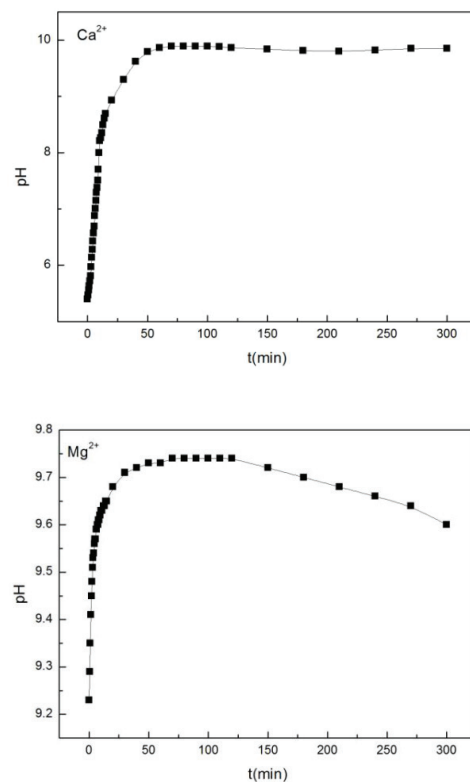


Fig. 9. Variations of pH in various adsorption processes ($[\text{Ca}^{2+}] = [\text{Mg}^{2+}] = 500 \text{ mg/L}$, $T = 35^\circ\text{C}$, LDOs = 1 g/L).

from the liquid phase, producing more single-sheet octahedral groups with positive charges. To balance the charge and maintain a stable structure, the anions were inserted to balance the charge and connect the laminates. Many layers combined with each other, along with the adsorption of Ca^{2+} and Mg^{2+} at the same time, restored the hydroxide structure. As the layer structure recovered, the adsorption of Ca^{2+} and Mg^{2+} increased.

To further investigate the mechanism of Ca^{2+} or Mg^{2+} adsorption by Mg–Al LDOs, the samples after adsorption were characterized by XRD, SEM and EDX. As evident from the XRD patterns of LDO-Ca and LDO-Mg shown in Fig. 10, the characteristic peaks of LDH ((003), (006), (012), (110)) appeared again, indicating that the collapse structure of LDH can recover during Ca^{2+} and Mg^{2+} adsorption from aqueous solutions.

The particle morphology of LDOs after Ca^{2+} and Mg^{2+} adsorption was investigated using the SEM images shown in Fig. 11. As can be seen in Fig. 11, the original layered structure with abundant flakiness with alveolate-like morphology was observed. Meanwhile, the chemical composition of LDO-R was analyzed using the corresponding EDX energy spectra. As can be seen from Fig. 12, the elemental basis (Mg, Al, C and O) for reconstructing the structure of LDHs compounds can be observed in the EDX spectra. Moreover, Ca element could also be observed, indicating the existence of Ca^{2+} in the structures of adsorbent.

The solution pH was greater than 7 during the adsorption of Mg^{2+} (alkaline environment), because Mg^{2+} is an element of hydroxide, and the adsorption of Mg^{2+} can be seen as the synthesis of hydroxide with the change in Mg/Al ratio. This process occurs in the alkaline environment. Therefore, adjusting the initial pH to alkaline is beneficial to the removal of Mg^{2+} . According to the calculation, the Mg^{2+} precipitates when the pH is about 10.5. Thus, the pH should be less than 10.5 to avoid direct precipitation. However, Ca^{2+} precipitation occurs at the pH of 12.05. Hence, the adsorption experiments can be carried out in the neutral environment, and do not require pH adjustment. The above results suggest that most Ca^{2+} was finally

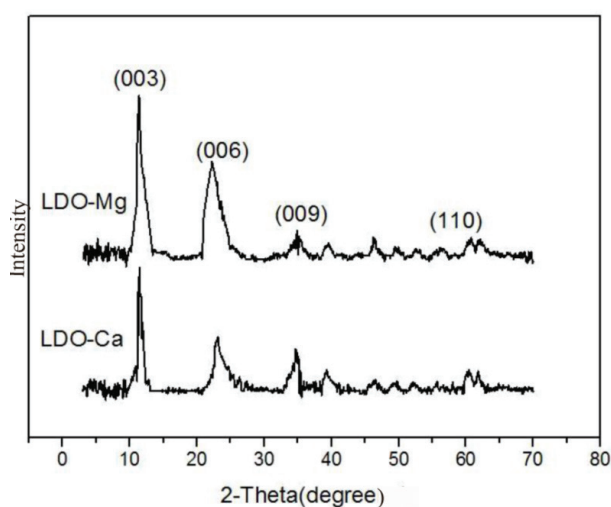


Fig. 10. X-ray diffraction patterns of LDO-Ca or LDO-Mg (after Ca^{2+} or Mg^{2+} adsorption on LDOs).

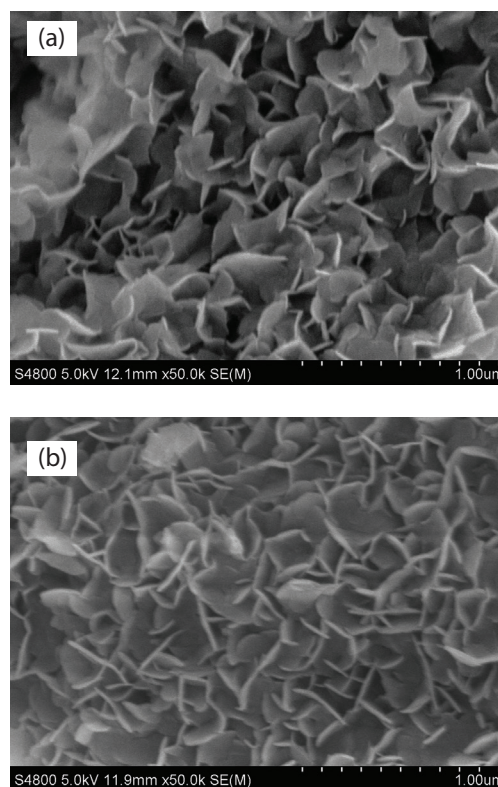


Fig. 11. The scanning electron microscopic (SEM) image of LDOs-Ca (a) or LDOs-Mg (b).

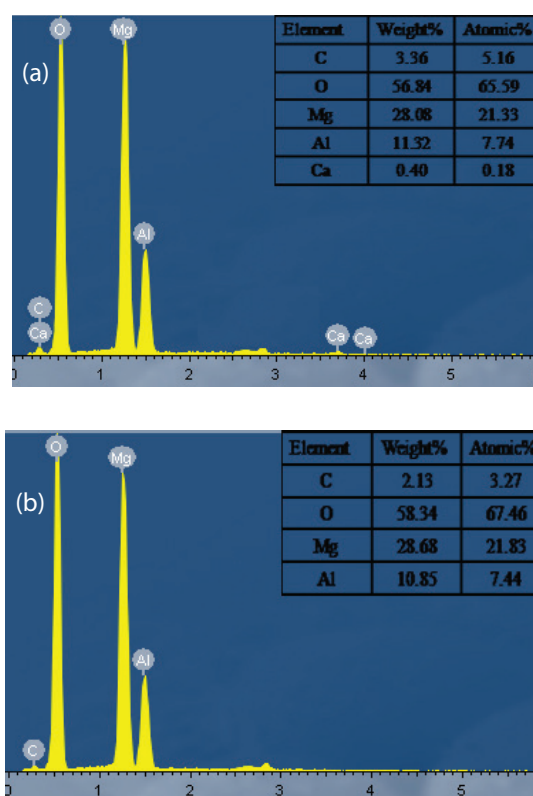


Fig. 12. The electron dispersive X-ray analysis (EDX) of LDOs-Ca (a) or LDOs-Mg (b).

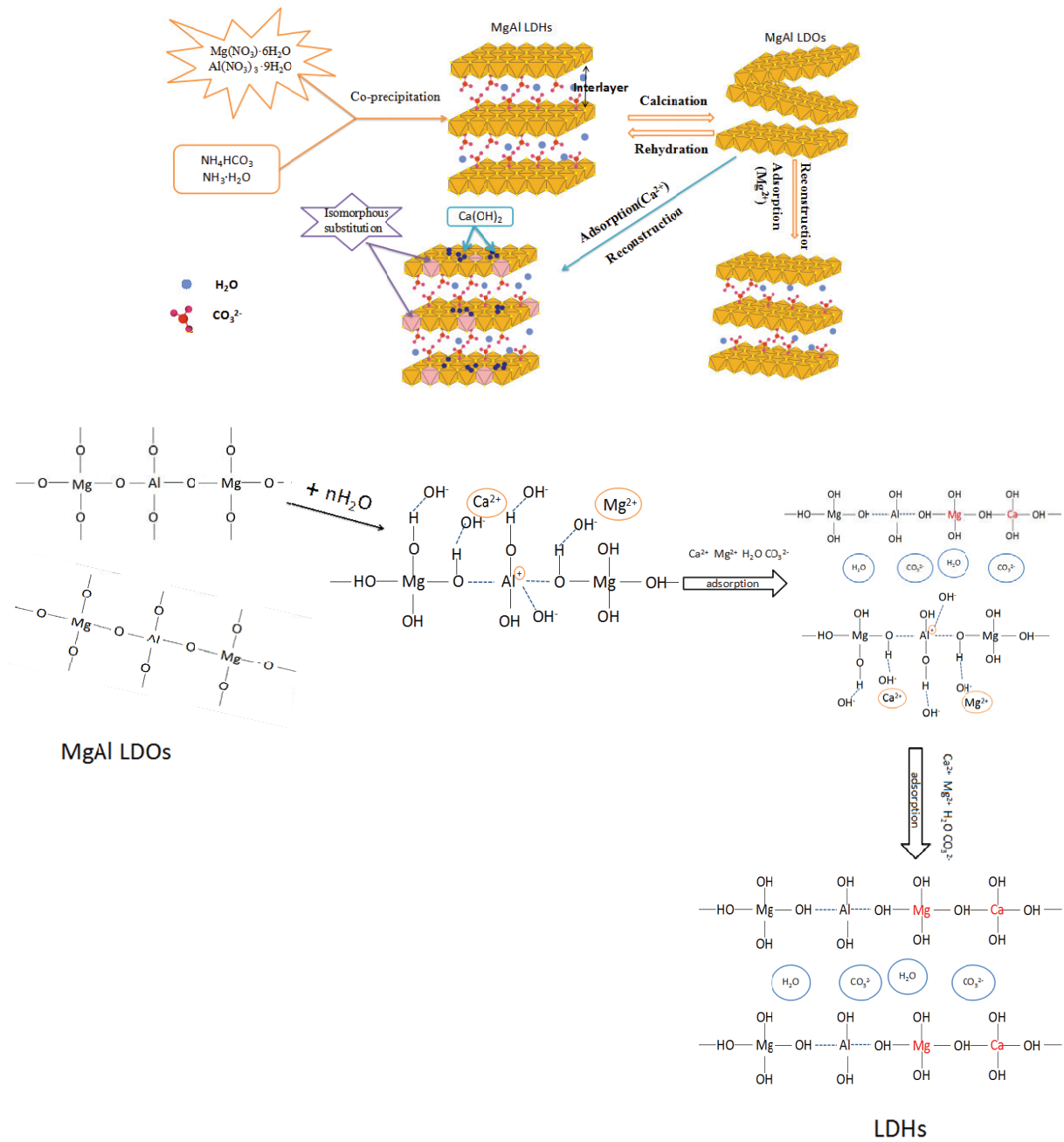


Fig. 13. The probable adsorptive mechanism between hardness ions (Ca^{2+} or Mg^{2+}) and MgAl LDOs.

removed on LDOs by the isomorphous substitution in the course of LDHs refactoring. The adsorption of Mg^{2+} occurred as the synthesis of hydrotalcite with the change of Mg/Al ratio.

4. Conclusions

In this study, an efficient Mg–Al LDOs adsorbent with significantly higher uptake capability for Ca^{2+} and Mg^{2+} was developed, by effectively utilizing the intrinsic adsorption characteristics of the LDOs material. As the layer structure of LDHs recovered, the adsorption of Ca^{2+} and Mg^{2+} increased. The results suggest that the adsorption

process was in accordance with the Langmuir isotherm model, and the thermodynamics parameters indicated that the Ca^{2+} or Mg^{2+} adsorption was spontaneous, irreversible and endothermic. The maximum Ca^{2+} and Mg^{2+} adsorption capacities were 305.31 and 105.99 mg/g, respectively. The pseudo-second-order kinetic model explained the adsorption reaction better. Moreover, the Ca^{2+} and Mg^{2+} activation energies were 25.099 and 20.167 kJ/mol, respectively, suggesting the possibility of chemical adsorption. The results of competitive adsorption on LDOs showed that the adsorption capacities are still high when Ca^{2+} and Mg^{2+} coexist in wastewater. Through repeated experiments,

Table 7
List of symbols in all equations

Symbols	Meaning
$q_{t,e}$ (mg/g)	The sorption capacity of adsorbent at the time t or equilibrium
C_0 (mg/L)	The initial concentration of Ca^{2+} and Mg^{2+}
$C_{t,e}$ (mg/L)	The concentration at t (min) or equilibrium
V (L)	The volume of solution
m (g)	The mass of LDOs
k_1 (min^{-1})	The rate constants of the pseudo-first-order models
k_2 (g/mg min)	The rate constants of the pseudo-second-order models
k_i (mg/g $\text{min}^{0.5}$)	The intraparticle diffusion rate constant
A g/(mg min)	The pre-exponential factor
E_a (kJ/mol)	The activation energy
R (8.314 J/mol·K)	Molar gas constant
T (K)	Absolute temperature
q_m (mg/g)	The maximum adsorption capacity
K_L (1/mg)	The Langmuir isotherm constant
K_F (mg/g)(L/mg) ^{1/n}	Freundlich constants
ΔG° (kJ/mol)	Changes in Gibbs free energy
ΔH° (kJ/mol)	Enthalpy
ΔS° (kJ/mol/K)	Entropy
K_D	The distribution coefficient

it was concluded that LDOs can be efficiently recycled to remove Ca^{2+} and Mg^{2+} . The removal percentage of Ca^{2+} and Mg^{2+} in actual desulfurization wastewater can reach more than 70% and the adsorbent can be used for the removal of hardness of ground water and industrial wastewater. Consequently, its performance indicates the potential use of this material in real-world applications.

Acknowledgments

The study was financially supported by Ministry of Science and Technology of China (2016YFE0112200), and Marie Skłodowska-Curie Actions (690958-MARSURISE-2015) and Independent Innovation Project of Important Key Technology, Shandong Province (No. 2014GJJS0501).

References

- [1] C. Necla, S. Eda Gokirmak, S. Ali, Removal of Cu(II) and Cd(II) ions from aqueous solutions using local raw material as adsorbent: a study in binary systems, *Desal. Wat. Treat.*, 75 (2017) 132–147.
- [2] S. Ma, J. Chai, G. Chen, W. Yu, S. Zhu, Research on desulfurization wastewater evaporation: present and future perspectives, *Renew. Sustain. Energy Rev.*, 58 (2016) 1143–1151.
- [3] B. Dou, W. Pan, Q. Jin, W. Wang, Y. Li, Prediction of SO_2 removal efficiency for wet flue gas desulfurization, *Energy Convers. Manage.*, 50 (2009) 2547–2553.
- [4] Z. Liang, L. Zhang, Z. Yang, T. Qiang, G. Pu, J. Ran, Evaporation and crystallization of a droplet of desulfurization wastewater from a coal-fired power plant, *Appl. Therm. Eng.*, 119 (2017) 52–62.
- [5] M. Barczak, K. Michalak-Zwierz, K. Gdula, K. Tyszczyk-Rotko, R. Dobrowolski, A. Dąbrowski, Ordered mesoporous carbons as effective sorbents for removal of heavy metal ions, *Microporous Mesoporous Mater.*, 211 (2015) 162–173.
- [6] C. Liu, X. Lei, L. Wang, J. Jia, X. Liang, X. Zhao, H. Zhu, Investigation on the removal performances of heavy metal ions with the layer-by-layer assembled forward osmosis membranes, *Chem. Eng. J.*, 327 (2017) 60–70.
- [7] S. Hao, A. Verlotta, P. Aprea, F. Pepe, D. Caputo, W. Zhu, Optimal synthesis of amino-functionalized mesoporous silicas for the adsorption of heavy metal ions, *Microporous Mesoporous Mater.*, 236 (2016) 250–259.
- [8] K. Mohamed, S. Zineb, H. Djamil, Removal of phosphate from industrial wastewater using uncalcined MgAl-NO_3 layered double hydroxide: batch study and modeling, *Desal. Wat. Treat.*, 57 (2016) 15920–15931.
- [9] H. Ji, W. Wu, F. Li, X. Yu, J. Fu, L. Jia, Enhanced adsorption of bromate from aqueous solutions on ordered mesoporous Mg–Al layered double hydroxides (LDHs), *J. Hazard. Mater.*, 334 (2017) 212–222.
- [10] X. Liang, Y. Zang, Y. Xu, X. Tan, W. Hou, L. Wang, Y. Sun, Sorption of metal cations on layered double hydroxides, *Colloids Surf., A*, 433 (2013) 122–131.
- [11] M. González, I. Pavlovic, R. Rojas-Delgado, C. Barriga, Removal of Cu^{2+} , Pb^{2+} and Cd^{2+} by layered double hydroxide–humate hybrid. Sorbate and sorbent comparative studies, *Chem. Eng. J.*, 254 (2014) 605–611.
- [12] Z.-Q. Zhang, H.-Y. Zeng, X.-J. Liu, S. Xu, C.-R. Chen, J.-Z. Du, Modification of MgAl hydrotalcite by ammonium sulfate for enhancement of lead adsorption, *J. Taiwan Inst. Chem. Eng.*, 60 (2016) 361–368.
- [13] Q. Guo, E.J. Reardon, Fluoride removal from water by meixnerite and its calcination product, *Appl. Clay Sci.*, 56 (2012) 7–15.
- [14] Y. Xiao, M. Sun, L. Zhang, X. Gao, J. Su, H. Zhu, The co-adsorption of Cu^{2+} and Zn^{2+} with adsorption sites surface-lattice reforming on calcined layered double hydroxides, *RSC Adv.*, 5 (2015) 28369–28378.
- [15] Y. Guo, Z. Zhu, Y. Qiu, J. Zhao, Enhanced adsorption of acid brown 14 dye on calcined Mg/Fe layered double hydroxide with memory effect, *Chem. Eng. J.*, 219 (2013) 69–77.
- [16] Y. Li, B. Gao, T. Wu, W. Chen, X. Li, B. Wang, Adsorption kinetics for removal of thiocyanate from aqueous solution by calcined hydrotalcite, *Colloids Surf., A*, 325 (2008) 38–43.
- [17] W. Ma, N. Zhao, G. Yang, L. Tian, R. Wang, Removal of fluoride ions from aqueous solution by the calcination product of Mg–Al–Fe hydrotalcite-like compound, *Desalination*, 268 (2011) 20–26.
- [18] Y. Shen, X. Zhao, X. Zhang, Removal of Cu^{2+} from the aqueous solution by tartrate-intercalated layered double hydroxide, *Desal. Wat. Treat.*, 57 (2016) 2064–2072.
- [19] G. Mascolo, M. Mascolo, On the synthesis of layered double hydroxides (LDHs) by reconstruction method based on the “memory effect”, *Microporous Mesoporous Mater.*, 214 (2015) 246–248.
- [20] N. Gerds, V. Katiyar, C.B. Koch, J. Risbo, D. Plackett, H.C.B. Hansen, Synthesis and characterization of laurate-intercalated Mg–Al layered double hydroxide prepared by coprecipitation, *Appl. Clay Sci.*, 65–66 (2012) 143–151.
- [21] M. Sun, J. Su, S. Liu, D. Wang, W. Yan, L. Zhang, Y. Xiao, X. Gao, Simultaneous removal of nickel and phosphorus from spent electroless nickel plating wastewater via calcined Mg–Al– CO_3 hydroxides, *RSC Adv.*, 5 (2015) 80978–80989.
- [22] C. Derradji, B. Abdallah, R. Abdelbaki, Removal of the anionic dye Biebrich scarlet from water by adsorption to calcined and non-calcined Mg–Al layered double hydroxides, *Desal. Wat. Treat.*, 57 (2016) 22061–22073.
- [23] Y. Li, B. Gao, T. Wu, D. Sun, X. Li, B. Wang, F. Lu, Hexavalent chromium removal from aqueous solution by adsorption on aluminum magnesium mixed hydroxide, *Water Res.*, 43 (2009) 3067–3075.
- [24] W. Wang, J. Zhou, G. Achari, J. Yu, W. Cai, Cr(VI) removal from aqueous solutions by hydrothermal synthetic layered double

- hydroxides: adsorption performance, coexisting anions and regeneration studies, *Colloids Surf., A*, 457 (2014) 33–40.
- [25] J. Wang, X. Wang, L. Tan, Y. Chen, T. Hayat, J. Hu, A. Alsaedi, B. Ahmad, W. Guo, X. Wang, Performances and mechanisms of Mg/Al and Ca/Al layered double hydroxides for graphene oxide removal from aqueous solution, *Chem. Eng. J.*, 297 (2016) 106–115.
- [26] S. Yu, X. Wang, Z. Chen, J. Wang, S. Wang, T. Hayat, X. Wang, Layered double hydroxide intercalated with aromatic acid anions for the efficient capture of aniline from aqueous solution, *J. Hazard. Mater.*, 321 (2017) 111–120.
- [27] F.L. Theiss, G.A. Ayoko, R.L. Frost, Iodide removal using LDH technology, *Chem. Eng. J.*, 296 (2016) 300–309.
- [28] L. Xiao, W. Ma, M. Han, Z. Cheng, The influence of ferric iron in calcined nano-Mg/Al hydrotalcite on adsorption of Cr(VI) from aqueous solution, *J. Hazard. Mater.*, 186 (2011) 690–698.
- [29] R.-r. Shan, L.-g. Yan, Y.-m. Yang, K. Yang, S.-j. Yu, H.-q. Yu, B.-c. Zhu, B. Du, Highly efficient removal of three red dyes by adsorption onto Mg–Al-layered double hydroxide, *J. Ind. Eng. Chem.*, 21 (2015) 561–568.
- [30] Y. Lin, Q. Fang, B. Chen, Perchlorate uptake and molecular mechanisms by magnesium/aluminum carbonate layered double hydroxides and the calcined layered double hydroxides, *Chem. Eng. J.*, 237 (2014) 38–46.
- [31] G. Huang, D. Wang, S. Ma, J. Chen, L. Jiang, P. Wang, A new, low-cost adsorbent: preparation, characterization, and adsorption behavior of Pb(II) and Cu(II), *J. Colloid Interface Sci.*, 445 (2015) 294–302.
- [32] M. Barnabas, S. Parambath, A. Mathew, S. Park, A. Vinu, C.-S. Ha, Highly efficient and selective adsorption of In^{3+} on pristine Zn/Al layered double hydroxide (Zn/Al-LDH) from aqueous solutions, *J. Solid State Chem.*, 233 (2016) 133–142.
- [33] Y. Shen, X. Zhao, X. Zhang, S. Li, D. Liu, L. Fan, Removal of Pb^{2+} from the aqueous solution by tartrate intercalated layered double hydroxides, *Korean J. Chem. Eng.*, 33 (2015) 159–169.
- [34] T. Kameda, J. Oba, T. Yoshioka, Recyclable Mg–Al layered double hydroxides for fluoride removal: kinetic and equilibrium studies, *J. Hazard. Mater.*, 300 (2015) 475–482.
- [35] C. Lei, X. Zhu, B. Zhu, C. Jiang, Y. Le, J. Yu, Superb adsorption capacity of hierarchical calcined Ni/Mg/Al layered double hydroxides for Congo red and Cr(VI) ions, *J. Hazard. Mater.*, 321 (2017) 801–811.
- [36] B. Tanhaei, A. Ayati, M. Lahtinen, M. Sillanpää, Preparation and characterization of a novel chitosan/ Al_2O_3 /magnetite nanoparticles composite adsorbent for kinetic, thermodynamic and isotherm studies of methyl orange adsorption, *Chem. Eng. J.*, 259 (2015) 1–10.
- [37] T. Anirudhan, S. Sreekumari, Adsorptive removal of heavy metal ions from industrial effluents using activated carbon derived from waste coconut buttons, *J. Environ. Sci.*, 23 (2011) 1989–1998.
- [38] Z. Yan, B. Zhu, J. Yu, Z. Xu, Effect of calcination on adsorption performance of Mg–Al layered double hydroxide prepared by a water-in-oil microemulsion method, *RSC Adv.*, 6 (2016) 50128–50137.
- [39] F. Ling, L. Fang, Y. Lu, J. Gao, F. Wu, M. Zhou, B. Hu, A novel CoFe layered double hydroxides adsorbent: high adsorption amount for methyl orange dye and fast removal of Cr(VI), *Microporous Mesoporous Mater.*, 234 (2016) 230–238.
- [40] M. Sui, Y. Zhou, L. Sheng, B. Duan, Adsorption of norfloxacin in aqueous solution by Mg–Al layered double hydroxides with variable metal composition and interlayer anions, *Chem. Eng. J.*, 210 (2012) 451–460.
- [41] Y. Ho, J. Ng, G. McKay, Kinetics of pollutant sorption by biosorbents: review, *Sep. Purif. Rev.*, 29 (2000) 189–232.
- [42] F. Yang, S. Sun, X. Chen, Y. Chang, F. Zha, Z. Lei, Mg–Al layered double hydroxides modified clay adsorbents for efficient removal of Pb^{2+} , Cu^{2+} and Ni^{2+} from water, *Appl. Clay Sci.*, 123 (2016) 134–140.
- [43] L. Zhong, X. He, J. Qu, X. Li, Z. Lei, Q. Zhang, X. Liu, Precursor preparation for Ca–Al layered double hydroxide to remove hexavalent chromium coexisting with calcium and magnesium chlorides, *J. Solid State Chem.*, 245 (2017) 200–206.
- [44] W. Yao, S. Yu, J. Wang, Y. Zou, S. Lu, Y. Ai, N.S. Alharbi, A. Alsaedi, T. Hayat, X. Wang, Enhanced removal of methyl orange on calcined glycerol-modified nanocrystalline Mg/Al layered double hydroxides, *Chem. Eng. J.*, 307 (2017) 476–486.
- [45] Y. Yang, N. Gao, W. Chu, Y. Zhang, Y. Ma, Adsorption of perchlorate from aqueous solution by the calcination product of Mg/(Al–Fe) hydrotalcite-like compounds, *J. Hazard. Mater.*, 209–210 (2012) 318–325.
- [46] Y. Yang, N. Gao, Y. Deng, S. Zhou, Adsorption of perchlorate from water using calcined iron-based layered double hydroxides, *Appl. Clay Sci.*, 65–66 (2012) 80–86.
- [47] M.G. Vieira, A.F. Neto, M.L. Gimenes, M.G. da Silva, Sorption kinetics and equilibrium for the removal of nickel ions from aqueous phase on calcined Bofe bentonite clay, *J. Hazard. Mater.*, 177 (2010) 362–371.
- [48] Q. Zhou, F. Chen, W. Wu, R. Bu, W. Li, F. Yang, Reactive orange 5 removal from aqueous solution using hydroxyl ammonium ionic liquids/layered double hydroxides intercalation composites, *Chem. Eng. J.*, 285 (2016) 198–206.
- [49] H. Zaghouane-Boudiaf, M. Boutahala, C. Tiar, L. Arab, F. Garin, Treatment of 2,4,5-trichlorophenol by MgAl–SDBS organo-layered double hydroxides: kinetic and equilibrium studies, *Chem. Eng. J.*, 173 (2011) 36–41.
- [50] T. Kameda, T. Yoshioka, T. Mitsunashi, M. Uchida, A. Okuwaki, The simultaneous removal of calcium and chloride ions from calcium chloride solution using magnesium–aluminum oxide, *Water Res.*, 37 (2003) 4045–4050.
- [51] P. Cai, H. Zheng, C. Wang, H. Ma, J. Hu, Y. Pu, P. Liang, Competitive adsorption characteristics of fluoride and phosphate on calcined Mg–Al– CO_3 layered double hydroxides, *J. Hazard. Mater.*, 213–214 (2012) 100–108.